Second harmonic autoresonant control of the $l=1$ diocotron mode in pure-electron plasmas

J. Fajans,[1] E. Gilson,[1] and L. Friedland[2]
[1]*Department of Physics, University of California, Berkeley, Berkeley, California 94720-7300*
[2]*Racah Institute of Physics, Hebrew University of Jerusalem, 91904 Jerusalem, Israel*
(Received 22 March 2000)

An oscillator whose frequency is amplitude dependent can be controlled by a drive whose frequency sweeps through a resonance with the oscillator's fundamental frequency. This phenomenon is called autoresonance, and has been previously investigated for drives with frequencies near the oscillator's fundamental or subharmonic frequencies. This paper examines autoresonance for drives at twice the fundamental frequency, i.e, second harmonic autoresonance. The $l=1$ diocotron mode in pure-electron plasmas, a very high Q nonlinear oscillator, is the focus of the paper. The theory for this oscillator is derived, and compared to experimental results. The results can be generalized to any Duffing-like driven nonlinear oscillator in which the coupling between the drive and the oscillator depends at least weakly on the oscillator amplitude.

PACS number(s): 52.25.Wz, 05.45.Xt, 52.35.Mw

I. INTRODUCTION

Adiabatic passage through a resonance in a driven nonlinear system may lead to persistent nonlinear phase locking (autoresonance) between the system and its drive, thereby engendering a strong and controllable system response. Autoresonance has many applications in particle accelerators [1], atomic physics [2,3], fluid dynamics [4], plasmas [5,6], and nonlinear waves [7,8]. Passage through the fundamental resonance in an initially quiescent nonlinear system necessarily yields phase locking [fundamental autoresonance (FAR)] when the driving amplitude exceeds a threshold proportional to $\alpha^{3/4}$, where α is the driving frequency sweep rate [4–6]. Recent studies also demonstrated subharmonic autoresonance or SHAR [9,10], via passage through an nth subharmonic of the fundamental frequency of the system. The mechanism for SHAR is different from that of FAR as it requires the self-generation of an internal nonlinear response that serves as an effective adiabatic drive. SHAR also has a threshold, which scales as $\alpha^{3/(4n)}$. Importantly, for both FAR and SHAR, the system enters autoresonance regardless of the initial driving phase when above threshold.

In the present work we study autoresonance by passage through a second harmonic resonance: we drive the system with a frequency that sweeps through twice the fundamental. We refer to this autoresonant phenomenon as 2HAR. As with FAR and SHAR, we shall show that there exists a driving amplitude threshold for 2HAR below which phase locking is impossible. However, unlike FAR and SHAR, this threshold does not scale as a simple power of the sweep rate, and beyond the threshold only a fraction of initial driving phases lead to phase locking. In further contrast to the FAR and SHAR, entering 2HAR by sweeping the driving frequency requires that the system be pre-excited to some initial amplitude. We study 2HAR experimentally and theoretically using the $l=1$ diocotron mode in pure electron plasmas [11] as a model system. Sec. II of this paper presents our experimental results, Sec. III describes the theory with the first part of this section concentrated on autoresonant state itself, and the second part concentrated on the transition into autoresonance. The last section presents our conclusions.

II. DIOCOTRON MODE EXPERIMENTS

The $l=1$ diocotron is a basic oscillating mode in pure-electron plasmas confined in a Malmberg-Penning trap [12]. These traps consist of a series of collimated conducting cylinders immersed in a strong, axial magnetic field **B**. The plasma forms a cylindrical column inside a center cylinder, and appropriately biased end cylinders provide longitudinal confinement. The axial magnetic field provides radial confinement. The $\mathbf{E}\times\mathbf{B}$ drifts that result from the plasma's self-electric field cause the plasma to rotate around itself (see Fig. 1). If the plasma is moved off center, it undergoes an additional $\mathbf{E}\times\mathbf{B}$ drift from the electric field of its image. As this drift always points azimuthally, the plasma orbits around the trap center. This motion, at frequency ω_D, is called the diocotron mode and is very stable, lasting for hundreds of thousands of rotations.

Assuming that the plasma column's charge per unit length is λ, then the electric field of its image, E, is approximately radial and constant across the plasma, $E\approx 2\lambda D/(R^2-D^2)$

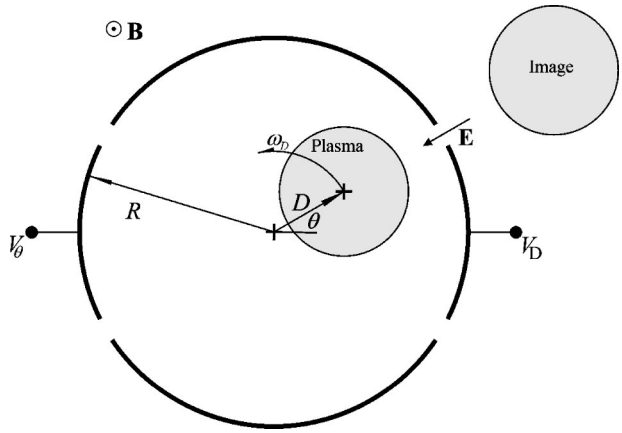

FIG. 1. End view of the trap showing the confining wall at radius R, the plasma at angle θ and distance D from the trap center, the plasma image, the image electric field **E**, and the diocotron drift at frequency $\omega/2\pi$. For our experiments, $\omega_0/2\pi=26.4\times10^3$ kHz. The mode is detected by monitoring the image charge on the pickup sector V_θ and driven by applying a voltage to the drive sector V_D. Further details are given in Ref. [6].

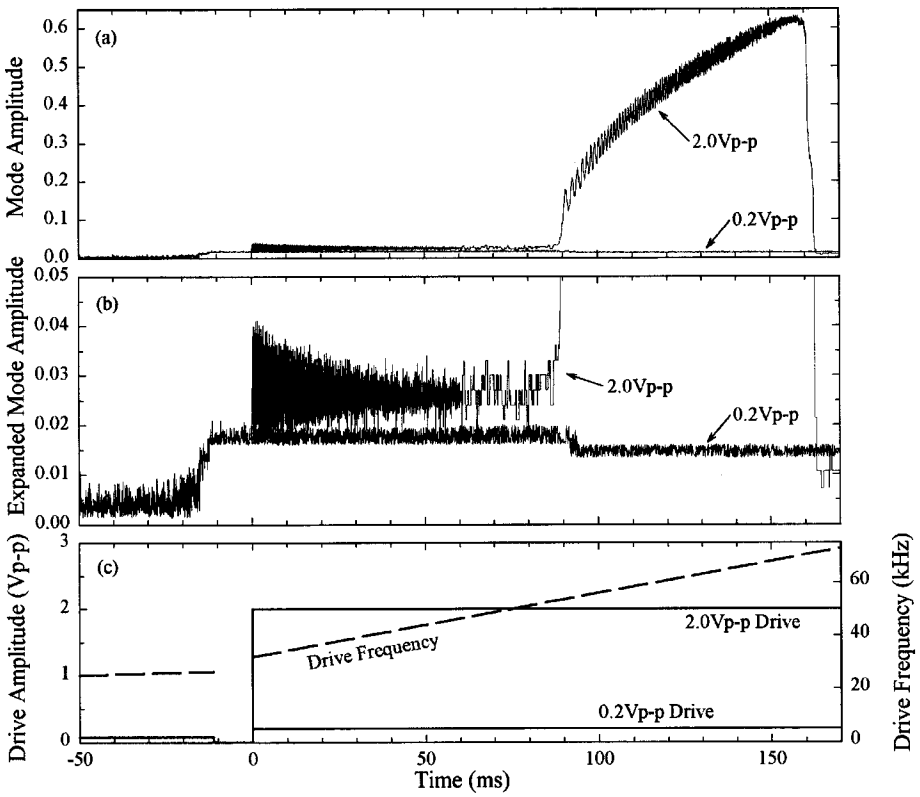

FIG. 2. Second harmonic excitation for a mode initially excited to $D/R=0.02$. (a) Mode amplitude D/R as a function of time for drives of 0.2 and 2.0 volts peak to peak (Vp-p). Only the 2.0 Vp-p drive is autoresonant. To show low amplitude details, both curves are replotted with an expanded scale in (b). When graphed with a finer time scale, the damped ''noise'' from 0 to 90 ms resolves into an amplitude oscillation with a frequency equaling the beat between the linear mode frequency and the drive frequency. (Digitization steps are visible from 60 to 90 ms in one of the expanded curves, as the diagnostic sensitivity was decreased there to cover the full mode amplitude.) (c) Drive amplitude (solid line) and drive frequency (dashed line) as a function of time. Note that the wave is preexcited by sweeping through the fundamental between -200 and -12 ms (the first 150 ms are not plotted); the second harmonic sweep occurs between 0 and 170 ms.

(cgs Gaussian units). Here R is the wall radius, and D is the offset of the plasma column from the center, i.e., the mode amplitude. The diocotron mode frequency ω_D follows by equating $\omega_D D$ to $c\mathbf{E}\times\mathbf{B}/B^2$, giving

$$\omega_D=\omega_0\left(\frac{1}{1-D^2/R^2}\right), \tag{1}$$

where $\omega_0=2c\lambda/BR^2$ is the linear resonant frequency. Note that the mode frequency increases with mode amplitude [13,14]. We can determine both the mode frequency and amplitude by measuring the image charge at a particular angle on the trap wall as a function of time. More precisely, we measure the time dependence of the surface charge on an azimuthal sector like the one labeled V_θ in Fig. 1. The received signal is calibrated to the displacement D by imaging the plasma on a phosphor screen at the end of the trap.

The experiments reported here were done at $B=1485$ G in a trap with wall radius $R=1.905$ cm. The plasma density was approximately 2×10^7 cm^{-3}, temperature $T=1$ eV, and plasma radius 0.6 cm. The measured linear diocotron frequency [15] was approximately 26.5 kHz. The plasma was confined within negatively biased cylinders separated by 10.25 cm. Finite length and plasma radius effects, discussed in Ref. [16], increase the linear frequency from that given by Eq. (1) by approximately 40% and also modify the dependence on D. We drive the diocotron mode by applying a signal to a driving sector V_{D}. [17] This driving signal creates electric fields which induce additional drifts.

Typical experimental results are given in Fig. 2. The mode is preexcited to $D/R=0.02$ by fundamental autoresonance: that is, by sweeping the frequency from 20 to 26.5 kHz. After a pause, the system is then driven at a frequency sweeping from 32 to 80 kHz. When this second sweep hits 53.0 kHz, twice the fundamental at 26.5 kHz, the mode amplitude follows the drive autoresonantly for the above-threshold 2.0 V peak-to-peak (Vp-p) drive, but not for the 0.2 Vp-p drive. For the autoresonant 2.0 Vp-p drive, the mode is phase locked to the drive at half the drive frequency; for the nonautoresonant 0.2 Vp-p drive, the mode and drive phases are uncorrelated.

III. PASSAGE THROUGH SECOND HARMONIC RESONANCE: THEORY

A. Second harmonic autoresonance

We model the $l=1$ diocotron mode driven by an external, second harmonic swept frequency drive by an approximate, isolated resonance Hamiltonian [18]

$$H(I,\theta,t)=-\omega_0\beta^{-1}\ln(1-\beta I)+\epsilon I\cos(2\theta-\varphi). \tag{2}$$

The angle variable θ is the angular position of the mode in

the trap, while $I=(D/R)^2$ is the normalized action. The factor β generalizes the unperturbed Hamiltonian to account for a broad class of finite plasma length and radius corrections [16]. For our experiments $\beta=0.6$. The complete driving potential is

$$V(D,\theta,t)=\mathrm{Re}\left[\sum_{l=0}^{\infty} A_l\left(\frac{D}{R}\right)^l \exp[i(l\theta-\varphi)]\right]V_p, \qquad (3)$$

where V_p is the peak-to-peak amplitude of the drive, A_l are the coupling coefficients determined by the sector geometry, $\varphi\equiv\int\omega(t)\,dt$ is the phase of the drive, and $\omega(t)$ is the instantaneous drive frequency. We assume that the driving frequency $\omega(t)=d\varphi/dt$ is swept linearly, i.e., $\omega(t)=2\omega_0+\alpha t$, and passes the second harmonic of the unexcited mode at $t=0$. Since $\omega(t)$ is generally near $2\omega_0$, we anticipate that only the second spatial harmonic of $V(D,\theta,t)$ can interact resonantly with the $l=1$ mode. Consequently only this harmonic is included in the Hamiltonian [Eq. (2)], and the appropriate drive amplitude is $\epsilon=2cA_2V_p\mathcal{C}/BR^2$. The parameter $\mathcal{C}$ accounts for finite length effects; the experimental geometry and other autoresonance experiments [6] indicate that $\mathcal{C}\approx0.187$ and $A_2=0.12$.

The Hamiltonian [Eq. (2)] yields the following system of equations for I and the phase mismatch $\Phi=2\theta-\varphi$:

$$dI/dt=2\epsilon I\sin\Phi, \qquad (4)$$

$$d\Phi/dt=\Lambda(I)-\alpha t+2\epsilon\cos\Phi, \qquad (5)$$

where $\Lambda(I)=2(\Omega-\omega_0)=2\omega_0\beta I/(1-\beta I)$ and $\Omega(I)=\omega_0/(1-\beta I)$ is the angular frequency of the diocotron mode. There exist two different time scales in our problem: the fast time scale $T_f=2\pi/\omega_0$ determined by the linear mode frequency ω_0, and the slow time scale $T_s=\alpha^{-1/2}$ associated with the driving frequency sweep rate. As we are interested in *slow* phase locked solutions in our system, we transform to the dimensionless time variable $\tau=t/T_s=\alpha^{1/2}t$, yielding the following dimensionless system:

$$dI/d\tau=\epsilon_0 I\sin\Phi, \qquad (6)$$

$$d\Phi/d\tau=QI/(1-\beta I)-\tau+\epsilon_0\cos\Phi, \qquad (7)$$

where Q is the ratio of the slow to fast time scales,

$$Q=4\pi T_s/T_f=2\omega_0\beta\alpha^{-1/2}\gg1,$$

and $\epsilon_0=2\epsilon\alpha^{-1/2}$ is the normalized drive amplitude.

For phase locked autoresonant evolution to occur, the system must be, at some initial time τ, in the vicinity of the quasi-steady-state solution $\overline{I}$, $\overline{\Phi}$ defined by setting the right-hand side of Eqs. (6) and (7) to zero:

$$\overline{\Phi}=\pi, \qquad (8)$$

$$Q\overline{I}/(1-\beta\overline{I})-\tau-\epsilon_0=0. \qquad (9)$$

If the system stays in the vicinity of this steady state, then, by Eq. (9), the action I will necessarily increase as the time τ increases, and the system will be in autoresonance. The system will indeed remain in this vicinity if (a) it begins in the vicinity of the quasi-steady-state, (b) $Q\overline{I}\gg1$ initially, and (c) the driving parameter ϵ_0 satisfies the double inequality

$$Q\overline{I}\gg\epsilon_0\gg(Q\overline{I})^{-1}. \qquad (10)$$

The left inequality in Eq. (10) allows us to neglect the small interaction term in Eq. (7) and rewrite it as $d\Phi/d\tau=QI/(1-\beta I)-\tau$. By differentiating this equation in time and substituting dI/dt from Eq. (6), we obtain

$$d^2\Phi/d\tau^2=\nu^2\sin\Phi-1, \qquad (11)$$

where $\nu^2\approx\epsilon_0Q\overline{I}/(1-\beta\overline{I})^2$. Now, if ν^2 varies *slowly* enough (see below), this equation describes the trajectory of a quasiparticle in a slowly varying, tilted cosine quasipotential

$$V_q(\Phi,\tau)=\Phi+\nu^2(\tau)\cos\Phi. \qquad (12)$$

Provided $\nu^2>1$, which is guaranteed by the right inequality in Eq. (10), this quasipotential will have definite wells; phase locking in our system corresponds to trapped quasiparticle oscillations in one of these wells.

The existence of potential wells is a necessary, but not sufficient, guarantee of phase lock. There are two possible ways to lose phase locking. The first would occur if the time variation of ν^2 were so fast that it violates the adiabaticity condition $\nu^{-2}d\nu/d\tau\ll1$. But

$$\nu^{-2}d\nu/d\tau=\frac{(1-\beta\overline{I})(1-\beta^2\overline{I^2})}{2Q\overline{I}(\epsilon_0Q\overline{I})^{1/2}}, \qquad (13)$$

where we have used $d\overline{I}/d\tau\approx Q^{-1}(1-\beta\overline{I})^2$, found by differentiating Eq. (9). Since both $\epsilon_0Q\overline{I}$ and $Q\overline{I}$ are large due to our initial conditions, $\nu^{-2}d\nu/d\tau\ll1$ and adiabaticity is preserved.

The second way to lose phase lock is through the adiabatic growth of the amplitude of the phase oscillations and the approach to the trapping separatrix as the slow parameter ν^2 increases in time. Here, we can use the action associated with the oscillations of the quasiparticle around the quasi-equilibrium, $J=\Delta\Phi\Delta I$, where $\Delta\Phi$ and ΔI are the amplitudes of the oscillations of Φ and I in the well. This action is conserved as ν varies adiabatically. But, from Eq. (6), $\Delta I=\epsilon_0\overline{I}\Delta\Phi/\nu_{osc}$, where ν_{osc} is the frequency of the quasiparticle oscillations. By using $\nu_{osc}\approx\nu$ as an estimate, we see that $\Delta\Phi=J/\Delta I\approx J\nu/\epsilon_0\overline{I}$. Since ν increases rapidly as $\beta\overline{I}$ approaches one, the oscillations $\Delta\Phi$ will also increase rapidly. The system will loose phase lock when $\Delta\Phi$ becomes of order π.

In summary, if the system is phase locked and in second harmonic autoresonance, it will remain in phase lock and in autoresonance until $\beta\overline{I}$ approaches one. How the system first gets into autoresonance is discussed next.

B. Trapping into resonance and the threshold condition

If the action $\overline{I}$ is below the ''well threshold'' action I_w defined by $\nu^2=\epsilon_0QI_w/(1-\beta I_w)^2\approx1$, the quasipotential wells [Eq. (12)] disappear. Consequently, if the system starts with an initial action I_0 that is less than the well threshold action I_w, the system will only enter autoresonance if the

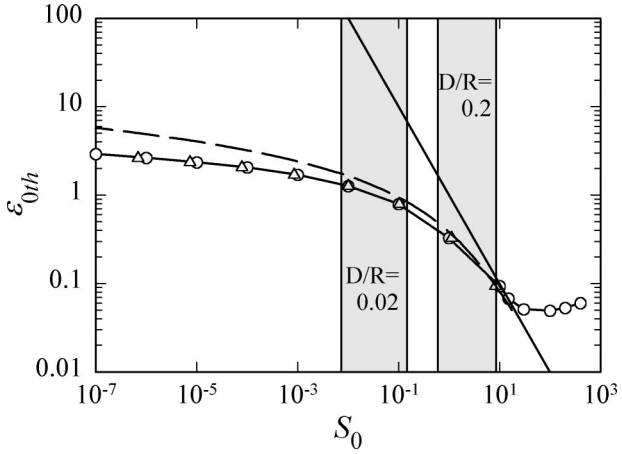

FIG. 3. Normalized threshold driving amplitude $\epsilon_{0th}=U(S_0)$ versus initial rescaled action S_0. (○), Data based on numerical solutions of system (14) and (15); (△), results by using formula Eq. (25); (dashed line) small ϵ_0 approximation Eq. (24); (tilted straight line) S_0^{-1}. The two grayed regions indicate the S_0 intervals used in the two measurements shown in Fig. 4, labeled by the initial value of D/R.

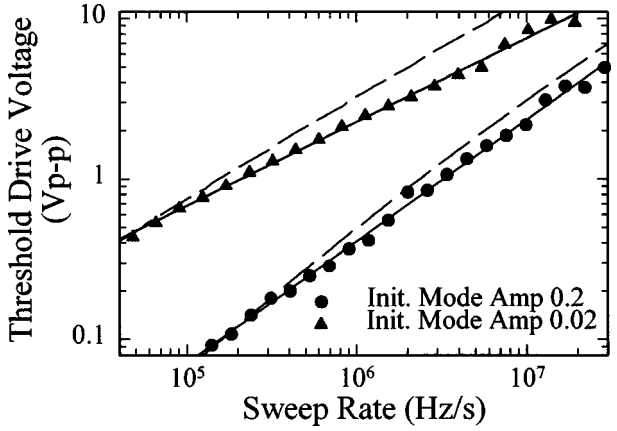

FIG. 4. Experimentally determined threshold drive voltage as a function of the sweep rate $\alpha/2\pi$, for two initial mode amplitudes D. As shown by the solid, best fit, lines, the drive voltage scales as the 0.76 and 0.52 power of the sweep rate for the $D/R=0.2$ and $D/R=0.02$ data, respectively. The dashed lines were obtained from the small ϵ_0 (small drive voltage) theory Eq. (24).

action grows to be greater than the well threshold action. Alternately, the initial action may be greater than the well threshold action, i.e., $I_0>I_w$. In this case the quasipotential wells exist initially and the quasiparticle is very likely to be free-streaming above the wells. Then the system can only enter autoresonance if the well depth increases fast enough to trap the quasiparticle in midflight, and the conditions for autoresonance are quite different than for $I_0<I_w$.

As the well threshold action is generally quite small, we will assume that $I_w\approx(\epsilon_0 Q)^{-1}\ll 1$. Then we can study trapping into resonance by rewriting system Eqs. (6) and (7) as

$$dS/d\tau=\epsilon_0 S\sin\Phi, \tag{14}$$

$$d\Phi/d\tau=S-\tau+\epsilon_0\cos\Phi, \tag{15}$$

where $S=QI$ is the scaled action. This is a single parameter (ϵ_0) system that must be solved subject to initial conditions $S=S_0=QI_0$ and $\Phi=\Phi_0=\Phi(-\infty)$. Despite their relative simplicity, Eqs. (14) and (15) still comprise a nonintegrable Hamiltonian system, so we proceed by investigating their solutions numerically. The solutions show that, as in FAR and SHAR, for a given S_0, phase locking (and subsequent autoresonance) is impossible for *all* initial phases when ϵ_0 is below a certain threshold value, ϵ_{0th}. Figure 3 shows (○) the numerically determined dependence $\epsilon_{0th}=U(S_0)$. The tilted straight line in Fig. 3 plots S_0^{-1}, and the slope of this line coincides with the largest (negative) slope of the threshold function $U(S_0)$. The two curves cross (i.e., $\epsilon_{0th}S_0=1$) at the inflection point $S_0\approx 10$ of $U(S_0)$. For S_0 well below the inflection point, say $S_0<0.1$, the slope of $U(S_0)$ in Fig. 3 is rather small. At higher values of S_0 the exponent γ of the local dependence $U\sim S_0^{-\gamma}$ increases and reaches the maximum value of $\gamma=1$ at the inflection point. Beyond the inflection point γ decreases rapidly and the threshold curve reaches its minimum of 0.05 at $S_0\approx 50$.

The form of the threshold curve $U(S_0)$ reflects the two different trapping mechanisms described in the first paragraph of this section. Consider the quasipotential Eq. (12), which, for $I\ll 1$, is

$$V_q=\Phi+\epsilon_0 S\cos\Phi. \tag{16}$$

Since the condition for this potential to have wells is $\epsilon_0 S>1$, and below the inflection point in Fig. 3 this condition is not met, the potential does not initially have wells. The potential wells appear only if, during the initial evolution stage, S increases beyond the value of ϵ_0^{-1}. Consequently there is a threshold drive amplitude for trapping, since ϵ_0 must be large enough for S to reach this value. In contrast, beyond the inflection point in Fig. 3, i.e., when $\epsilon_0 S_0>1$, the quasipotential wells exist initially and, as mentioned above, the quasiparticle is very likely to free-stream above the wells. The system can only enter autoresonance if the well depth increases fast enough to trap the quasiparticle in midflight.

Let us briefly return to our original parameters α, ϵ, and I_0. Since $\epsilon_0=2\epsilon\alpha^{-1/2}$, we have

$$\epsilon_{th}(\alpha,I_0)=\frac{1}{2}\alpha^{1/2}U(2\beta\omega_0\alpha^{-1/2}I_0). \tag{17}$$

Therefore,

$$\epsilon_{th}(k^2\alpha,kI_0)=k\epsilon_{th}(\alpha,I_0), \tag{18}$$

and we can obtain the threshold $\epsilon_{th}(k^2\alpha,kI_0)$ from $\epsilon_{th}(\alpha,I_0)$ for any value k.

We can compare some of these predictions with our experimental results. Figure 4 shows the experimental threshold versus the sweep rate for two initial amplitudes of the diocotron mode, $D/R=0.02$ and 0.2 ($I_0=0.0004$ and 0.04, respectively). We find that, to a good approximation, the thresholds scale as $\epsilon_{th}\sim\alpha^{0.52}$ and $\epsilon_{th}\sim\alpha^{0.76}$ in the two cases. The two curves lie in the two relatively narrow intervals $0.0073<S_0<0.15$ and $0.59<S_0<8.5$. In the first interval (for $D/R=0.02$), the power dependence of $U(S_0)$ is rather

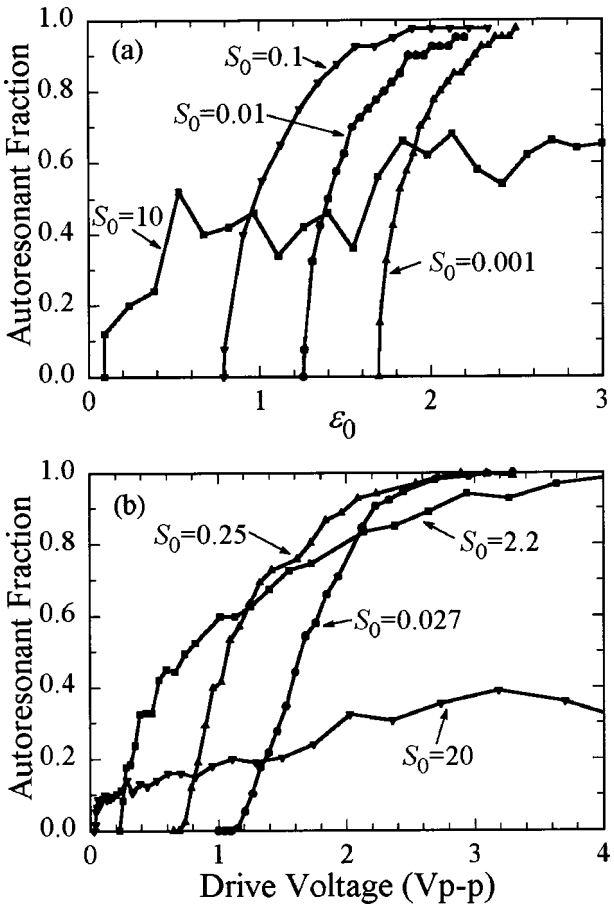

FIG. 5. (a) The fraction of the initial $\Phi_0 \in [0,2\pi]$, which yield phase locking and autoresonance, as a function of the driving amplitude ϵ_0 for $S_0=0.001$, 0.01, 0.1, and 10. The form of the fraction curve changes near the inflection point at $S_0 \approx 10$ in Fig. 3. (b) Experimental data demonstrating qualitatively similar behavior, taken at $\alpha=1.508\times10^6$ rad/s^2. For comparison, a peak-to-peak drive voltage of 1 Vp-p would correspond to $\epsilon_0 \approx 1.36$.

weak, roughly $U \sim S_0^{-0.20} \sim \alpha^{0.1}$; therefore, $\epsilon_{th} \sim \alpha^{0.60}$ by Eq. (17), in fair agreement with the experimental scaling. In the second interval ($D/R=0.2$), the function U varies faster with S_0, and scales approximately as $U \sim S_0^{-0.48} \sim \alpha^{0.24}$. Thus, $\epsilon_{th} \sim \alpha^{0.74}$, in good agreement with the experiment. Note that, as mentioned earlier, the largest exponent γ of the scaling $U \sim S_0^{-\gamma}$ is $\gamma=1$, in which case $U \sim S_0^{-1} \sim \alpha^{1/2}$. This happens at the inflection point, where one encounters the fastest scaling $\epsilon_{th} \sim \alpha^{1/2} U \sim \alpha$.

As with FAR and SHAR, autoresonance in 2HAR is impossible below the drive threshold. Unlike FAR and SHAR, where above the threshold the system enters autoresonance regardless of the initial phase of the system, in 2HAR only a fraction of the initial phases Φ_0 yield autoresonance. For example, Fig. 5(a) shows the percentage of the initial $\Phi_0 \in [0,2\pi]$ leading to autoresonance as a function of ϵ_0 for $S_0=0.001$, 0.01, 0.1, and 10. For the lower three values of S_0 (and for any smaller values of S_0,) the fraction of the initial phases that enter autoresonance increases with ϵ_0, and approaches 100%. The value $S_0=10$, however, is near the inflection point of $U(S_0)$, and consequently near where the quasipotential wells are initially present. For this value of S_0 the fraction of autoresonance phases reaches only $\sim$60%, illustrating another difference between starting with or without initial quasipotential wells. Similar behavior is observed experimentally [Fig. 5(b)].

To complete our understanding of the threshold phenomenon and the reasons behind the incomplete trapping of initial phases in the system, we examine the initial evolution in the system Eqs. (14) and (15) in more detail. We shall limit ourselves to the parameter region where $S_0 < S_w = QI_w = \epsilon_0^{-1}$, i.e, the region in which the quasipotential initially does not have potential wells. Here S must *increase* from its initial value S_0 to S_w for trapping to occur. Nonetheless, we can approximate S by S_0 in Eq. (15) without significantly changing the trapping physics; thus, Eq. (15) becomes $d\Phi/d\tau = S_0 - \tau + \epsilon_0 \cos\Phi$. Furthermore, the constant S_0 in this last equation can be removed by shifting the time τ, so that the full system of equations for studying the initial excitation is

$$dS/d\tau = \epsilon_0 S \sin\Phi, \tag{19}$$

$$d\Phi/d\tau = -\tau + \epsilon_0 \cos\Phi. \tag{20}$$

The evolution of Φ in this system is decoupled from S; thus, simple integration yields

$$S = S_0 \exp(\epsilon_0 F), \tag{21}$$

where the function

$$F(\Phi_0, \epsilon_0, \tau) = \int_{-\infty}^{\tau} \sin\Phi(\tau')\, d\tau' \tag{22}$$

is fully determined by the solution of Eq. (20) for Φ subject to the initial condition Φ_0 and the value of the parameter ϵ_0.

In the limit $\epsilon_0 \to 0$, the solution of Eq. (20) reduces to $\Phi(t) = \Phi_0 + \tau^2/2$, and F can be found analytically:

$$F(\Phi_0, \epsilon_0 \to 0, \tau \to \infty) = \sqrt{\pi}(\sin\Phi_0 - \cos\Phi_0). \tag{23}$$

This function has a maximum value at $\Phi_0 = 3\pi/4$, namely, $\sqrt{2\pi}$, at which point S will likewise attain its maximum value, $S_0 \exp(\sqrt{2\pi}\epsilon_0)$. Since S must exceed the well threshold value $S_w = \epsilon_0^{-1}$ for the quasiparticle to be trapped, the threshold drive ϵ_{0th} as a function of the initial amplitude S_0 can be determined from the equation

$$\epsilon_{0th}^{-1} = S_0 \exp(\sqrt{2\pi}\epsilon_{0th}), \tag{24}$$

valid in the limit $\epsilon_{0th} \to 0$. We plot this formula in Fig. 3, and, as expected, it agrees well with the numerical solution of the original system [Eqs. (14) and (15)] for small ϵ_0.

The threshold drive ϵ_{0th} is sufficient only for the optimal initial angle, $\Phi_0 = 3\pi/4$. When ϵ_0 is increased beyond ϵ_{0th}, an ever larger set of other initial angles Φ_0 become autoresonant as their values of $S = S_0 \exp[F(\Phi_0, \epsilon_0, t)\epsilon_0]$ exceed $1/\epsilon_0$. Clearly F cannot be negative if S is to grow. It might appear from Eq. (23) that half the initial angles would lead to negative F. The derivation of Eq. (23), however, ignores the influence of the ϵ_0 term in Eq. (20). This term favors angles $\Phi(t)$ that pull the integrand in Eq. (22) positive, and makes the function F positive for most, but not all, initial angles Φ_0. For example, the exact solution for F is shown in Fig. 6 for $\epsilon_0=1$ and 20 evenly spaced initial $\Phi_0 \in [0,2\pi]$. In all cases, F asymptotes to a fixed value, most of which are posi-

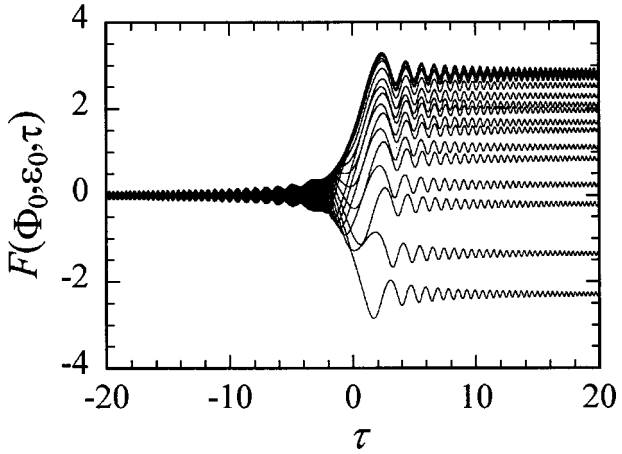

FIG. 6. The evolution of the response function $F(\Phi_0,\epsilon_0,\tau)$ for $\epsilon_0=1$ and for 20 evenly spaced initial $\Phi_0\in[0,2\pi]$. Most Φ_0 yield positive asymptotic values of $F(\Phi_0,\epsilon_0,\tau)$, but some yield negative values. Note that integrating between $\tau=-20$ (not $-\infty$) and $+20$, as is done in this figure, is sufficient for illustrating the asymptotic picture.

tive. For a few initial phases, however, the asymptote is negative. Such phases will not be trapped even for values of ϵ_0 much larger than ϵ_{0th}.

A more general estimate for the threshold than Eq. (24) can be found by numerically scanning over all the initial phases for the maximum value, F_m, of F as a function of ϵ_0. Then for every ϵ_0, the threshold S_{0th} can be found from the relation

$$S_{0th}=\epsilon_0^{-1}\exp(-\epsilon_0 F_m). \tag{25}$$

This last expression shows that, as expected, a finite initial excitation is necessary for entering 2HAR by passage through resonance. One can also view Eq. (25) as yielding the threshold driving amplitude $\epsilon_{0th}=U(S_0)$ or $\epsilon_{th}=\epsilon_{th}(\alpha,I_0)$ for a given I_0. Equation (25), plotted in Fig. 3, is in very good agreement with the results of the original system [Eqs. (14) and (15)] for all S_0 below the inflection point.

IV. CONCLUSIONS

We can extract a relatively simple picture that accounts for most of the important features of 2HAR. Since only the second spatial harmonic of the drive can interact with the mode resonantly, and since the fields from this mode disappear at the origin, the mode will not interact with the drive if the mode is on-axis. Thus, 2HAR cannot occur unless the mode is preexcited. When the drive frequency crosses twice the mode's linear resonant frequency, the mode receives a ''kick'' that may make its amplitude large enough for the mode to be trapped in a quasipotential well. If so, it will stay in resonance with the drive and grow to large amplitude: the system is in second harmonic autoresonance. The kick amplitude required for 2HAR depends on the size of the initial excitation, the sweep rate, and the drive amplitude, and the amplitude requirement leads to a threshold criterion. Near the threshold, the phase difference between the initial wave and the drive must lie in a narrow band for 2HAR. As the threshold is exceeded, an ever larger band of initial phase differences is acceptable, and eventually virtually all initial phase differences lead to 2HAR. Alternately, the initial mode amplitude may be large enough that the quasipotential wells exists from the very beginning. In this case, 2HAR will only occur when the mode is dynamically trapped into the wells. This process is less robust, and not all initial phase differences will enter into resonance.

In this paper, we have studied second harmonic autoresonance (2HAR) in the context of the $l=1$ diocotron equation. However, 2HAR will occur in any Duffing-like driven oscillator system so long as the coupling between the mode and the drive has component that depends on the drive amplitude. Such a component assures that there can exist a resonant interaction at the mode's fundamental frequency.

ACKNOWLEDGMENTS

This work was supported by the US-Israel Binational Science Foundation and the Office of Naval Research.

[1] M. S. Livingston, *High-energy Particle Accelerators* (Interscience, New York, 1954).
[2] B. Meerson and L. Friedland, Phys. Rev. A **41**, 5233 (1990).
[3] W.K. Liu, B. Wu, and J.M. Yuan, Phys. Rev. Lett. **75**, 1292 (1995).
[4] L. Friedland, Phys. Rev. E **59**, 4106 (1999).
[5] J. Fajans, E. Gilson, and L. Friedland, Phys. Rev. Lett. **82**, 4444 (1999).
[6] J. Fajans, E. Gilson, and L. Friedland, Phys. Plasmas **6**, 4497 (1999).
[7] I. Aranson, B. Meerson, and T. Tajima, Phys. Rev. A **45**, 7500 (1992).
[8] L. Friedland and A.G. Shagalov, Phys. Rev. Lett. **81**, 4357 (1998).
[9] L. Friedland, Phys. Rev. E **61**, 3732 (2000).
[10] L. Friedland, J. Fajans, and E. Gilson, Phys. Plasmas (to be published).
[11] J.H. Malmberg, C.F. Driscoll, B. Beck, D.L. Eggleston, J. Fajans, K. Fine, X.P. Huang, and A.W. Hyatt, in *Non-Neutral Plasma Physics*, edited by C.W. Roberson and C.F. Driscoll, AIP Conf. Proc. 175 (AIP, New York, 1988), p. 28.
[12] J.H. Malmberg and J.S. deGrassie, Phys. Rev. Lett. **35**, 577 (1975).
[13] S.A. Prasad and J.H. Malmberg, Phys. Fluids **29**, 2196 (1986).
[14] K.S. Fine, Phys. Fluids B **4**, 3981 (1992).
[15] The experiments reported here were taken at slightly different trap parameters than the experiments reported earlier in Ref. [5]. These differences, together with long term drifts in the trap, account for the slight differences in the reported frequencies and critical drives.
[16] K.S. Fine and C.F. Driscoll, Phys. Plasmas **5**, 601 (1998).
[17] In the experiment the receiving and driving sectors do not extend the full length of the plasma, and are separated axially to reduce coupling.
[18] R. Chu, J.S. Wurtele, J. Notte, A.J. Peurrung, and J. Fajans, Phys. Fluids B **5**, 2378 (1993).